DOES VARIABILITY PLAY A ROLE IN HAMSTRING STRAIN INJURIES? A PILOT STUDY IN SPRINTING

Carlie J. Ede, Glen M. Blenkinsop and Sam J. Allen

School of Sport, Exercise and Health Sciences, Loughborough University, UK

A scaled OpenSim model was used to assess the variability and changes in muscle loads across multiple strides and at different running speeds (2-8 $m \cdot s^{-1}$). Peak biceps femoris muscle fibre force, length, velocity and power occurred during the late swing phase of running and became more variable above 6 $m \cdot s^{-1}$. With each increase in running speed from 2-8 $m \cdot s^{-1}$, peak force occurred earlier in the swing, at longer muscle lengths and became less variable in its timing.Changes in variability can create a greater risk of injury and exploring these trends further may provide additional insight into hamstring strain injuries.

KEYWORDS: Musculoskeletal modelling, muscle force, muscle injury, running

INTRODUCTION: Hamstring strain injury (HSI) is one of the leading causes of injury and time away from many competitive sports (Opar, Williams, & Shield, 2012). The majority of HSI occur at or near maximal running velocity, with the biceps femoris long head (BFlh) the most common site of injury (Askling, Tengvar, Saartok, & Thorstensson, 2007). Despite a growing body of research, little change has been observed in the prevalence of HSI, suggesting knowledge of hamstring aetiology may be incomplete (Opar et al., 2012). Musculoskeletal (MSK) models can assist in the understanding of muscle function, providing insight into the cause and prevention of HSI. Using these methods, peak hamstring force and strain have been identified during the late swing phase of running (Chumanov, Heiderscheit, & Thelen, 2007; Dorn, Schache, & Pandy, 2012; Schache, Dorn, Blanch, Brown, & Pandy, 2012; Thelen, Chumanov, Best, Swanson, & Heiderscheit, 2005) and suggested as risk factors for HSI. However, the mechanisms behind HSI still remain unclear (Opar et al., 2012). Additionally, these conclusions are commonly made from the analysis of a single stride, neglecting the possible role of variability on HSI. Even within skilled sportspeople, every time the same movement is performed a certain degree of change may be recorded (Preatoni et al., 2013). As an individual approaches maximal speed, small variations in coordination can result in large changes to muscle function, increasing the risk of movements exceeding safe physical limits. Using a 3-dimensional MSK model, Chumanov et al. (2007) noted that a 0.1% perturbation to muscle forces resulted in excessive stretch within the BFlh, highlighting the sensitivity to neuromuscular changes and the need to better understand the role of variability during running and the possible links with HSI. Therefore, the aim of this study was to assess the variability and changes in muscle loads across multiple strides at different running speeds. It was expected that muscle load will increase with running speed, but also that it would become more variable as an individual approached maximal velocity.

METHODS: One male participant (age: 41 years height: 1.75 m mass: 74.3 kg), who was physically active and free from injury, completed multiple running trials on a high-speed instrumented treadmill (3DI, Treadmetrix, Utah, USA) following informed consent and university ethical approval. Synchronised force (1000 Hz) and 3-D kinematics (500 Hz, 16 Vicon Vantage cameras, Vicon, Oxford Metrics Ltd., Oxford, UK) were recorded at 2, 4, 6 and 8 $m \cdot s^{-1}$. Three 10 s trials were recorded during 2 mins of running at the lower two speeds, which were used as a warmup for the later trials. At the higher speeds the treadmill was mounted at speed and a minimum of 10 strides were recorded, with three trials recorded at 6 $m \cdot s^{-1}$ and one recorded at 8 $m \cdot s^{-1}$. Sufficient rest was provided between each trial. The raw voltage data from the four triaxial force transducers within the instrumented treadmill were calibrated using an inverted sensitivity matrix and combined to calculate the ground reaction force. Foot ground contact was identified from the vertical force using a 100 N threshold. The

raw voltage data was then filtered during ground contact using a 4th order low pass Butterworth filter with a 20 Hz cut-off, with the voltages during the flight phase set to zero. The ground reaction force, centre of pressure and free moment were then re-calculated from the filtered voltages.

A generic OpenSim model (Lai, Arnold, & Wakeling, 2017) comprising 22 segments, 37 degrees of freedom, 80 muscle-tendon actuators of the lower limbs and 17 ideal torque actuators to control the torso and upper limbs, was scaled to the participant using the ratio of experimental markers placed on anatomical landmarks during a static trial, and the distance of the same markers placed on the model. Joint angle time histories were calculated using OpenSim's inverse kinematic pipeline and the output filtered with a 4th order low pass Butterworth filter (20 Hz cut-off). The kinematics and ground reaction forces were then combined using the inverse dynamics pipeline to determine the net joint moments. Muscle fibre length was determined from OpenSim's muscle analysis tool and numerically differentiated to give muscle fibre velocity. The individual muscle fibre forces were calculated using static optimisation, which minimises the sum of the square of muscle activations, for each recorded running stride (defined as right foot touchdown to right foot touchdown). The static optimisation was constrained to follow the muscle force-length-velocity relationship. Residual actuators were added to the pelvis to account for dynamic inconsistencies in the inverse dynamics solution. Coordinate actuators were also added to the lower limbs but assigned a low force value so that high activations were required for their use and penalised in the cost function. Muscle force was then multiplied by muscle fibre velocity to give muscle power, so that positive power represented concentric contractions and negative power represented eccentric contractions.

All recorded trials were processed and analysed, each trial was divided into full stride cycles with only the right limb analysed. The first and last strides were discarded to ensure a consistent gait pattern. All strides were split into stance and swing phases (Figure 1) and time normalised (1001 data points) to represent 0-100% of each phase. The mean and standard deviation were then calculated for each running speed, along with peak values and timings of the muscle force, velocity and power. All data was processed using a custom Matlab script (R2018a, MathWorks. Inc, MA, USA).

RESULTS: 23 strides at 2 m·s^{-1}, 27 strides at 4 m·s^{-1}, 26 strides at 6 m·s^{-1} and 9 strides at 8 m·s^{-1} were analysed. At 2 m·s^{-1} the average peak vertical ground reaction force was 2.53 BW (± 0.05 BW) and increased to 3.74 BW (± 0.22 BW) at 8 m·s^{-1}. During stance the BFlh worked concentrically with peak length, velocity, force and power occurring at or close to foot contact for all running speeds (Figure 1). Peak muscle force and power in stance showed the greatest variation at 6 m·s^{-1} (Table 1) but remained similar in magnitude between speeds. A small increase in peak muscle velocity was also observed with increased running speed (Table 1).

During the swing phase the BFlh first shortened, before achieving peak length towards the end of the swing (Figure 1). Peak muscle velocity increased from 0.28 m·s^{-1} (2 m·s^{-1}) to 1.27 m·s^{-1} (8 m·s^{-1}). Peak muscle force occurred towards the end of the swing phase (Figure 1), approximately doubling in magnitude with each speed increment from 4 m·s^{-1} (632 N ± 44 N), to 6 m·s^{-1} (1473 N ± 134 N), and 8 m·s^{-1} (2649 N ± 81 N), resulting in a high eccentric load. Muscle power also showed a large increase in both magnitude and variability between 6 and 8 m·s^{-1} (Table 1). Additionally, as running speed increased the timing of peak muscle force became less variable, occurred earlier in the swing phase [2 m·s^{-1}: 95.8% ± 4.2% (± 22 ms) vs. 8 m·s^{-1}: 70.0% ± 0.8% (± 3 ms)] and at longer muscle lengths (Table 1).

DISCUSSION: The aim of this study was to assess the variability and changes in muscle load across multiple strides and running speeds. In line with past research, this study found that peak BFlh load (length, velocity, force and power) increased with running speed. During stance the BFlh was shown to work concentrically, with peak force occurring during the terminal swing

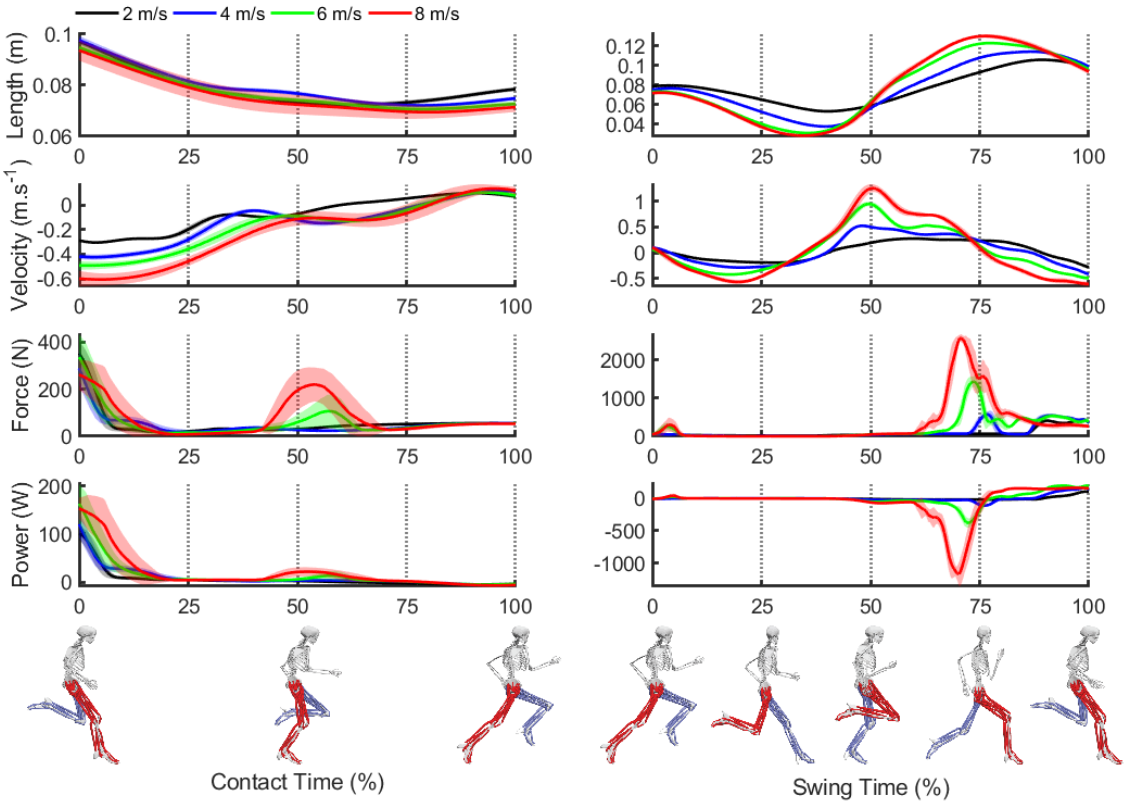

Figure 1: Muscle fibre length, velocity, force and power (from top to bottom) of the biceps femoris long head for the different running speeds. Solid lines show the average of all strides with the standard deviation (shaded area). Negative power represents eccentric contraction. Graphic of running represents the phases of the gait cycle (right leg in red) matched to the vertical dashed lines.

phase as the muscle lengthened, resulting in a high eccentric load (Figure 1 and Table 1). During the swing phase, this load became more variable above 6 $m \cdot s^{-1}$, but interestingly, the timing of the peak force became less variable and occurred earlier in the swing as running speed increased (Figure 1).

Peak muscle force (35.65 $N \cdot kg^{-1}$, 8 $m \cdot s^{-1}$) is higher than those previously reported by Schache et al. (2012) (26.35 $N \cdot kg^{-1}$, 8.95 $m \cdot s^{-1}$) and Chumanov et al. (2007) (21.4 $N \cdot kg^{-1}$, 8.64 $m \cdot s^{-1}$) during overground and treadmill running, respectively. During stance, Schache et al. (2012) also reported a BFlh force of 4.61 $N \cdot kg^{-1}$, which compares well with the results found here (4.05 $N \cdot kg^{-1}$). The variability of muscle loads across multiple strides has not been previously reported; as running speed increased, the peak muscle force occurred earlier in the swing phase, at longer muscle lengths and showed less variability in its timing (Figure 1 and Table 1). It is possible that to match the increasing force demands as running speed increases, the range of muscle lengths at which peak force can occur safely is reduced. Sudden changes in variability, as a result of coordination errors or external factors could result in high muscle loads occurring at longer muscle lengths, increasing the risk of injury (Hamill, Palmer, & Van Emmerik, 2012). Exploring this trend in larger groups and at higher velocities may help to provide further insight into the understanding of HSI.

MSK modelling is a powerful tool that can provide insight into the function and prevention of muscular injuries. Although scaled to the participant, the effects of using a generic model and parameters, and the use of static optimisation methods must be considered when evaluating the results. Static optimisation is limited by its simplified muscle dynamics, ignoring tendon compliance and parallel elastic elements of muscle, however, it provides the computational efficiency required to assess the variability over multiple strides and has been shown to produce similar results to dynamic optimisation methods (Anderson & Pandy, 2001).

CONCLUSION: Understanding the mechanisms behind muscular injuries is key to the prevention and treatment of HSI. In line with past research, peak muscle length, velocity, force and power was shown to increase with running speed, although in a novel finding, the variability in the timing of these peak loads was reduced. Variation outside these small ranges may then result in large changes and potential injury to the muscle, especially as an individual approaches maximal velocity. The role of variability in HSI has received little attention in the past, exploring these trends further may assist in understanding the causes and prevention of HSI.

Table 1: mean (± std) muscle fibre length at peak force and peak muscle fibre force, velocity and power of the biceps femoris long head during different running speeds. Negative velocity represents muscle shortening, positive velocity represents muscle lengthening. Negative Power represent eccentric contraction, positive power represents concentric contraction.

	Length at peak force (m)	Force (N)	Velocity ($m \cdot s^{-1}$)	Power (W)
		Stance		
2 $m \cdot s^{-1}$	0.097 ± 0.001	355 ± 52	-0.31 ± 0.01	103 ± 14
4 $m \cdot s^{-1}$	0.098 ± 0.002	289 ± 72	-0.43 ± 0.02	121 ± 27
6 $m \cdot s^{-1}$	0.095 ± 0.002	336 ± 97	-0.5 ± 0.03	163 ± 41
8 $m \cdot s^{-1}$	0.081 ± 0.013	301 ± 48	-0.61 ± 0.04	154 ± 23
		Swing		
2 $m \cdot s^{-1}$	0.102 ± 0.003	453 ± 35	0.28 ± 0.01	110 ± 11
4 $m \cdot s^{-1}$	0.111 ± 0.002	632 ± 44	0.53 ± 0.03	173 ± 13
6 $m \cdot s^{-1}$	0.121 ± 0.001	1473 ± 134	0.96 ± 0.04	-414 ± 52
8 $m \cdot s^{-1}$	0.124 ± 0.002	2649 ± 81	1.27 ± 0.07	-1296 ± 118

REFERENCES

Anderson, F. C., & Pandy, M. G. (2001). Static and dynamic optimization solutions for gait are practically equivalent. *Journal of Biomechanical Engineering*, *34*, 153–161.

Askling, C. M., Tengvar, M., Saartok, T., & Thorstensson, A. (2007). Acute first-time hamstring strains during high-speed running: A longitudinal study including clinical and magnetic resonance imaging findings. *American Journal of Sports Medicine*, *35*(2), 197–206.

Chumanov, E. S., Heiderscheit, B. C., & Thelen, D. G. (2007). The effect of speed and influence of individual muscles on hamstring mechanics during the swing phase of sprinting. *Journal of Biomechanics*, *40*(16), 3555–3562.

Dorn, T. W., Schache, A. G., & Pandy, M. G. (2012). Muscular strategy shift in human running: dependence of running speed on hip and ankle muscle performance. *Journal of Experimental Biology*, *215*(13), 2347–2347.

Hamill, J., Palmer, C., & Van Emmerik, R. E. A. (2012). Coordinative variability and overuse injury. *Sports Medicine, Arthroscopy, Rehabilitation, Therapy and Technology*, *4*(1), 1–9.

Lai, A. K. M., Arnold, A. S., & Wakeling, J. M. (2017). Why are Antagonist Muscles Co-activated in My Simulation? A Musculoskeletal Model for Analysing Human Locomotor Tasks. *Annals of Biomedical Engineering*, *45*(12), 2762–2774.

Opar, D. A., Williams, M. D., & Shield, A. J. (2012). Hamstring strain injuries: Factors that Lead to injury and re-Injury. *Sports Medicine*, *42*(3), 209–226.

Preatoni, E., Hamill, J., Harrison, A. J., Hayes, K., van Emmerik, R. E. A., Wilson, C., & Rodano, R. (2013). Movement variability and skills monitoring in sports. *Sports Biomechanics*, *12*(2), 69–92.

Schache, A. G., Dorn, T. W., Blanch, P. D., Brown, N. A. T., & Pandy, M. G. (2012). Mechanics of the human hamstring muscles during sprinting. *Medicine and Science in Sports and Exercise*, *44*(4), 647–658.

Thelen, D. G., Chumanov, E. S., Best, T. M., Swanson, S. C., & Heiderscheit, B. C. (2005). Simulation of biceps femoris musculotendon mechanics during the swing phase of sprinting. *Medicine and Science in Sports and Exercise*, *37*(11), 1931–1938.